Habits of Magnetosome Crystals in Coccoid Magnetotactic Bacteria

Ulysses Lins,[1]* Martha R. McCartney,[2] Marcos Farina,[3] Richard B. Frankel,[4] and Peter R. Buseck[5]

Instituto de Microbiologia Professor Paulo de Góes, Universidade Federal do Rio de Janeiro, Rio de Janeiro, Brazil[1]; Center for Solid State Science, Arizona State University, Tempe, Arizona[2]; Instituto de Ciências Biomédicas, Universidade Federal do Rio de Janeiro, Rio de Janeiro, Brazil[3]; Department of Physics, California Polytechnic State University, San Luis Obispo, California[4]; and Departments of Geology and Chemistry/Biochemistry, Arizona State University, Tempe, Arizona[5]

High-resolution transmission electron microscopy and electron holography were used to study the habits of exceptionally large magnetite crystals in coccoid magnetotactic bacteria. In addition to the crystal habits, the crystallographic positioning of successive crystals in the magnetosome chain appears to be under strict biological control.

Magnetotactic bacteria (MB) contain magnetosomes comprising nanoscale magnetic iron mineral crystals in membrane vesicles (1). A striking feature of magnetosome magnetite crystals is that they have different, but consistent, projected shapes in different bacterial species or strains when observed by transmission electron microscopy (TEM) (3). The overall sizes of the crystals, the width/length ratios, and the relative sizes of putative corner faces can vary from one bacterial species or strain to another, resulting in the distinctive projected shapes.

Off-axis electron holography can be used to obtain both magnetic and structural information about nanometer-sized magnetic crystals (4). We report here on the application of electron holography and high-resolution TEM to study the crystal habits of magnetosomes in two coccoid morphotypes of MB collected from a brackish lagoon at Itaipu, Brazil, which is located on the coast north of Rio de Janeiro (10). Itaipu-1 and Itaipu-3 bacteria predominated in the lagoon at the time the samples for the present study were collected. Itaipu-1, the largest coccoid organism, contains two chains of magnetosomes (Fig. 1); the magnetosome crystals have roughly square projections, lengths up to 250 nm, and width/length ratios of ca. 0.9 (10). These are the largest-volume magnetosome crystals yet reported. Itaipu-3 has magnetosome crystals that are elongated (width/length ratio of ~0.6) along [111], with lengths up to 120 nm and prominent corner facets. Whereas magnetosomes in most MB, including Itaipu-3, are permanent single-magnetic domains, we previously reported that the large magnetosomes in Itaipu-1 are metastable, single-magnetic domains (9).

Cells were isolated from sediment and water samples by using glass chambers with capillary ends positioned inside magnetic coils (8). Whole cells, or magnetosomes extracted from disrupted cells (see reference 9 for details), were deposited on holey-carbon TEM grids. Water drops containing the crystals were spread over the grids. Grids were then air dried and observed under a transmission electron microscope. In some cases the crystal suspension was sonicated prior to deposition on the grids. The disruption process resulted in Itaipu-1 and Itaipu-3 magnetosomes mixed together on the TEM grid (Fig. 2). High-resolution TEM, selected-area electron diffraction measurements, and off-axis electron holography were made with a Phillips CM200 FEG TEM operated at 200 kV. For details on the application of electron holography to MB, see references 4 and 9.

Figure 2 shows a chain of magnetosomes from Itaipu-1, together with some smaller, more elongated, crystals from Itaipu-3. The inset in Fig. 2A is a $[2\bar{1}\bar{1}]$ microdiffraction pattern from the second large Itaipu-1 crystal indicated by the arrow; the inset in Fig. 2B is a $[1\bar{1}0]$ microdiffraction pattern from the same Itaipu-1 crystal, following tilting of the chain 30° about the chain axis. Microdiffraction of the other Itaipu-1 crystals in the chain show they are all oriented with [111] axes of elongation along the chain direction and are all in [110] projection, indicating rigid rotational alignment of the crystals about [111]

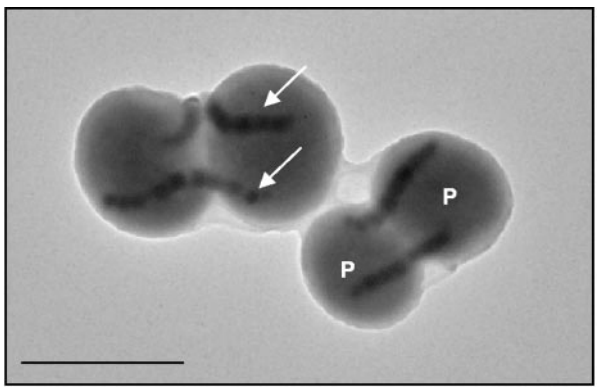

FIG. 1. TEM image of two Itaipu-1 cocci. Each bacterium has two chains of magnetosomes (arrows) and two phosphorus-rich globules (P). Scale bar, 1 μm.

* Corresponding author. Mailing address: Departamento de Microbiologia Geral, Instituto de Microbiologia Prof. Paulo de Góes, CCS, Bl. I, Universidade Federal do Rio de Janeiro, 21941-590, Rio de Janeiro, RJ, Brazil. Phone: (55)21-2562-6738. Fax: (55)21-2560-8344. E-mail: ulins@micro.ufrj.br.

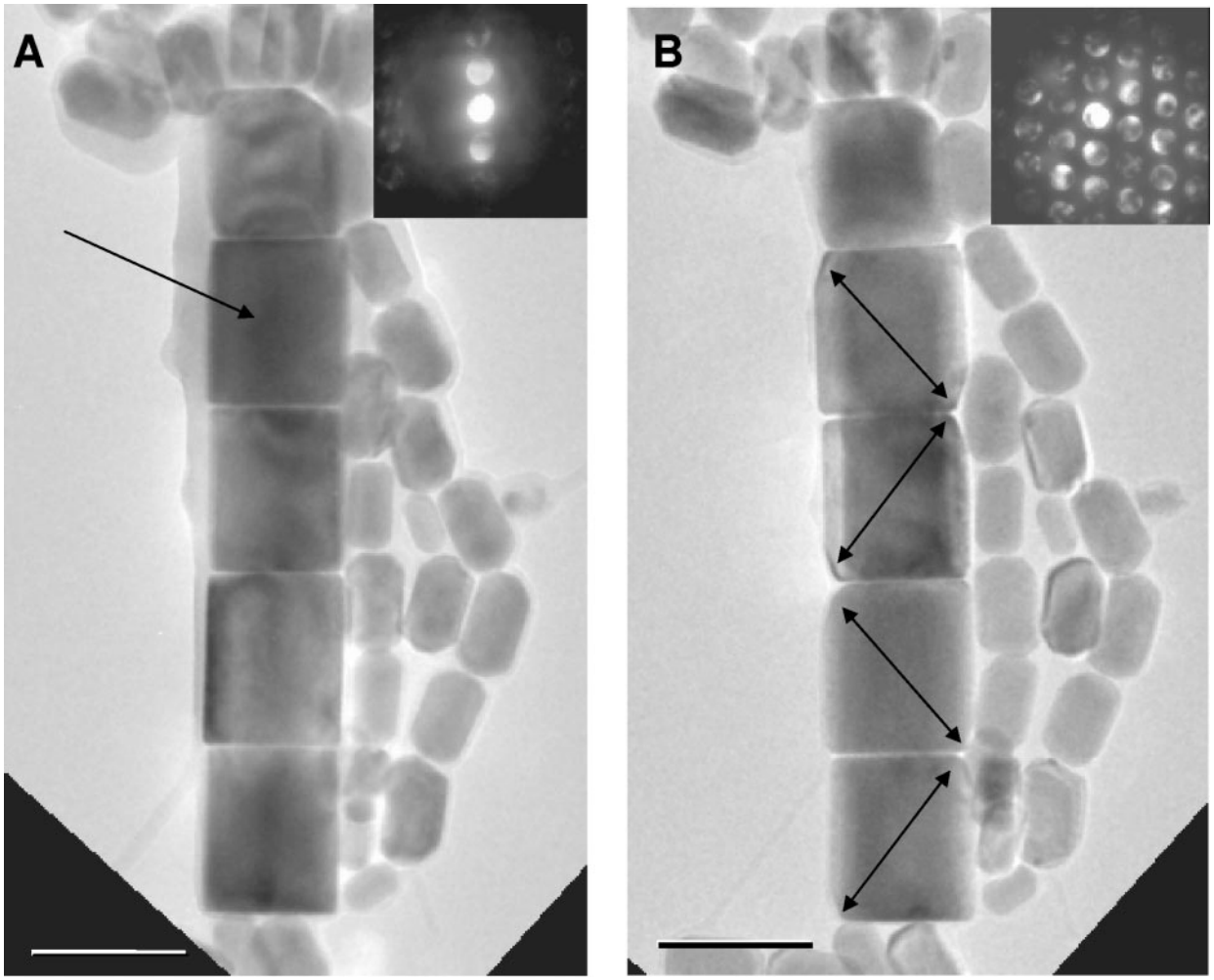

FIG. 2. TEM images of Itaipu-1 and Itaipu-3 magnetosomes. (A) Chain of large magnetosomes from magnetotactic bacterial strain Itaipu-1 surrounded by smaller, elongated magnetosomes from strain Itaipu-3. The inset is a [211] diffraction pattern from the second large Itaipu-1 crystal (arrow). (B) Same chain as in panel A tilted 30° about the [111] axis. The inset [110] diffraction pattern from the second large Itaipu-1 crystal shows (111) fringes from the magnetically easy axis. Corner faces {111} and {200} are mirrored about the vertical (or horizontal) axis for alternating crystals (double arrows); see detailed image in Fig. 3. Scale bar, 200 nm.

in the chain. Figure 3 shows a high resolution image of a crystal in $[1\bar{1}0]$ projection; the high-resolution images of each of the corners (indicated by arrows) shows the planes that apparently bound the crystal. It is remarkable that the crystals in this chain are not only all aligned with [111] elongation axes and $[1\bar{1}0]$ axes parallel but also ordered with like corner faces of adjacent crystals facing each other.

It is not possible to tell from the two-dimensional images alone whether any set of lattice fringes is parallel to terminating facets or wedge edges. Whereas the darker contrast in the centers of the crystals may indicate that the crystals are thicker there, the contrast of TEM images is an unreliable indicator of thickness and thus cannot be used to determine morphology (2). Therefore, off-axis electron holography was used to determine the cross-sectional thickness of the crystals perpendicular to the [111] elongation axis.

Figure 4 shows the electrostatic phase contributions calculated from the electron holography data (not shown), presented as thickness contours. The thickness profiles, along the lines in Fig. 4A and B indicated by the arrow crossing the thickness contours of one Itaipu-1 and one Itaipu-3 crystal, are given in Fig. 4C, where half-thickness is plotted with distance along the arrow.

The profiles for both orientations of the Itaipu-1 crystals are consistent with a crystal hexagonal cross section perpendicular to [111] and consistent with theoretical models of elongated magnetite crystals shown in reference 3. In the $[1\bar{1}0]$ projection, a $(1\bar{1}0)$ face is perpendicular to the beam in the center, with adjacent $(0\bar{1}1)$ and $(10\bar{1})$ faces at 60° at either side, giving a "flat-top" profile. In the $[2\bar{1}\bar{1}]$ projection, the intersection between (110) and (101) faces is perpendicular to the beam and adjacent $(0\bar{1}1)$ and $(01\bar{1})$ faces parallel to the beam, giving a "tent-top" profile. The profiles are also consistent with the greater thickness of the Itaipu-1 crystal compared to Itaipu-3, as expected from the projected images. The Itaipu-3 crystals in

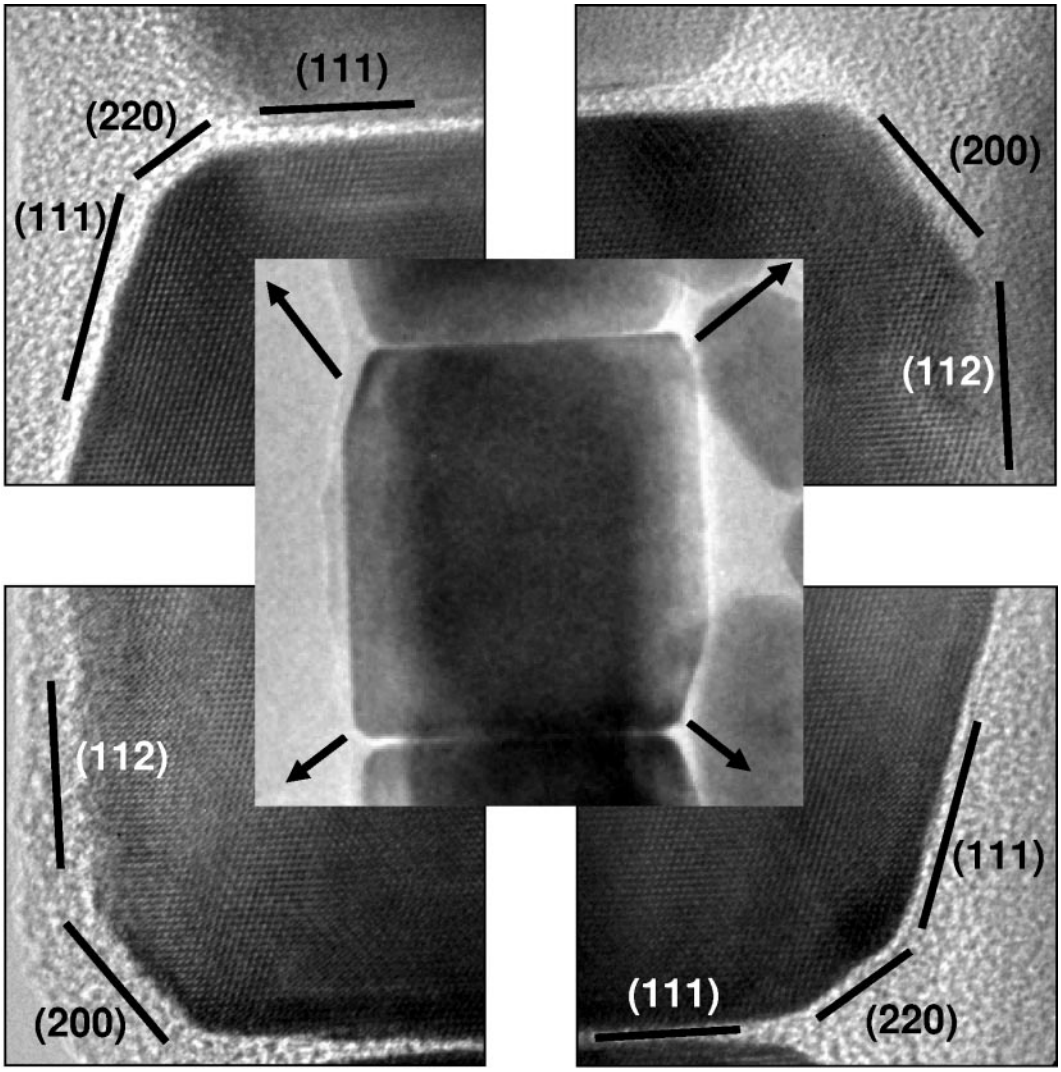

FIG. 3. High-resolution TEM images of Itaipu-1 magnetosomes with indexed bars parallel to lattice planes. Obvious symmetries between even the very small facets on opposite sides of the crystal diagonals can be seen. Comparison with other crystals of the chain in Fig. 2 also indicates that this symmetry regularly alternates between crystals.

this figure have random orientations in both sets of images and show an "average" thickness profile.

Our results confirm that both Itaipu-1 and Itaipu-3 bacteria have magnetosome magnetite crystals with similar elongated, nonequidimensional, crystal habits, although the sizes of the crystals and their width to length ratios differ. Interestingly, the chain from Itaipu-1 (shown in Fig. 2) reveals a particular spatial arrangement of the magnetosomes along the chain. This pattern of assembly of magnetosomes is not random, indicating that there is strictly controlled positioning of the crystals along the magnetosome chain. This organization pattern could be used as a biomarker in studies of nanometer crystals of magnetite isolated from soils, sedimentary deposits, or meteorites.

The functional significance of the large volume of the magnetite crystals in Itaipu-1 is unclear. The fact that other coccoid MB at Itaipu have smaller magnetosomes demonstrates that the large magnetosomes in Itaipu-1 are not necessary for magnetotaxis in the anomalously low magnetic field (0.25 G) of the South Atlantic that includes Itaipu. Moreover, as shown in reference 9, the larger magnetosomes do not have the optimal magnetic dipole moment per unit volume because of the persistence of magnetic vortex states. Nevertheless, a calculation of the total magnetic dipole moment for an Itaipu-1 cell shown in Fig. 1, assuming a pseudohexagonal prismatic habit for the magnetite crystals, results in an mB/k_BT value of $\sim$250, i.e., greater by more than a factor of 10 than the value required for efficient magnetotaxis in 0.25 G (5), suggesting other functions of the magnetosomes in Itaipu-1.

Itaipu-1 bacteria occur in a continuous size distribution varying from 1.4 to 3.5 μm (10). A plot of the largest dimension of the bacteria versus the length of their largest magnetosomes indicates a direct relation between these two parameters (10). In addition, whole-cell hybridization with the universal probe EUB338, which binds to all bacteria, shows a low rRNA con-

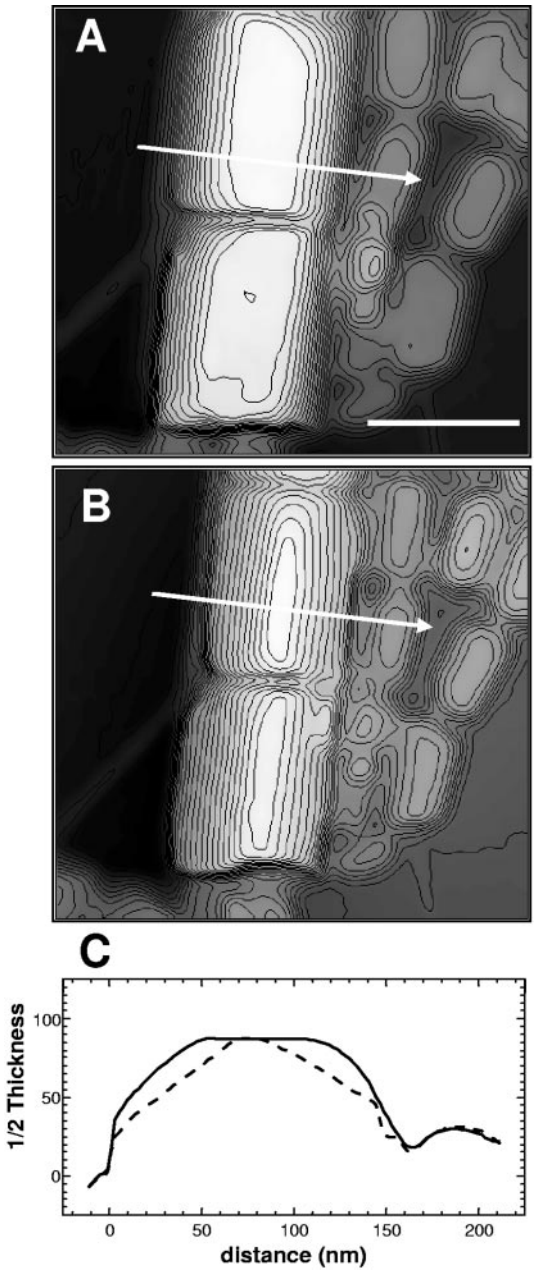

FIG. 4. (A) Electrostatic contribution to the holographic phase shift from the Itaipu magnetosomes shown in Fig. 2, oriented to a [110] projection. The contours represent the projected thickness and show a flat-topped morphology and steep sides. (B) Projected thickness contours for the same crystals after tilting by 30° about the chain axis to a [211] orientation. The contours show that the crystal is much thicker along its center than along its edges, having a central ridge formed by intersecting faces. (C) Line profiles (solid line for panel A and dashed line for panel B) across the magnetosomes from the indicated positions (arrows), converted to values of one-half their thickness, reveal a 120° angle between the facets for the [211] projection, which is consistent with the intersection of [110] faces. Scale bar, 150 nm (panels A and B).

tent for Itaipu bacteria, indicating a slow growth rate. Therefore, the continuous size distribution may represent different stages of slow growth of a single phylogenetically defined population, which would allow time for the largest crystals to form. The parallel observation that Itaipu-4 bacteria (10), which also synthesize unusually large crystals (although these crystals are smaller than Itaipu-1 magnetosomes), are more closely related to Itaipu-3 bacteria than Itaipu-1 (10), further indicates that the ability to produce unusually large magnetosomes is not characteristic for a distinct phylogenetic lineage within the MB.

The relative volume occupied by the magnetosomes in Itaipu-1 and the fact that additional iron is associated with the large phosphorous-rich granules in the cells (7) means that this organism accumulates an unusually large amount of iron (by a factor of 50 or so) compared to some other MB such as *Magnetospirillum magnetotacticum*. This suggests that iron might play a role as energy source or electron sink or as an intermediate in energy metabolism (6) in Itaipu-1. It would be interesting to have this organism in pure culture to evaluate the effects of various concentrations of oxygen, iron, and specific iron chelators on magnetosome growth.

P.R.B. acknowledges support from U.S. National Science Foundation grant CHE 9714101. M.F. and U.L. acknowledge support from the Brazilian CNPq.

Electron microscopy was performed at the Center for High Resolution Electron Microscopy at Arizona State University. U.L. thanks P.R.B. for the opportunity to spend time at Arizona State University to work on the manuscript.

REFERENCES

1. **Bazylinski, D. A., and R. B. Frankel.** 2004. Magnetosome formation in prokaryotes. Nat. Rev. Microbiol. **2:**217–230.
2. **Buseck, P. R., R. E. Dunin-Borkowski, B. Devouard, R. B. Frankel, M. R. McCartney, P. A. Midgley, M. Posfai, and M. Weyland.** 2001. Magnetite morphology and life on Mars. Proc. Natl. Acad. Sci. USA **98:**13490–13495.
3. **Devouard, B., M. Posfai, X. Hua, D. A. Bazylinski, R. B. Frankel, and P. R. Buseck.** 1998. Magnetite from magnetotactic bacteria: size distributions and twinning. Am. Mineralogist **83:**1387–1399.
4. **Dunin-Borkowski, R. E., M. R. McCartney, M. Posfai, R. B. Frankel, D. A. Bazylinski, and P. R. Buseck.** 2001. Off-axis electron microscopy of magnetotactic bacteria: magnetic microstructure of strains MV-1 and MS-1. Eur. J. Mineral. **13:**671–684.
5. **Frankel, R. B.** 1984. Magnetic guidance of organisms. Annu. Rev. Biophys. Bioeng. **13:**85–103.
6. **Guerin, W. F., and R. P. Blakemore.** 1992. Redox cycling of iron supports growth and magnetite synthesis by *Aquaspirillum magnetotacticum.* Appl. Environ. Microbiol. **58:**1102–1109.
7. **Lins, U., and M. Farina.** 1999. Phosphorous-rich granules in uncultured magnetotactic bacteria. FEMS Microbiol. Lett. **172:**23–28.
8. **Lins, U., F. Freitas, C. N. Keim, H. Lins de Barros, D. M. S. Esquivel, and M. Farina.** 2003. Simple homemade apparatus for harvesting uncultured magnetotactic microorganisms. Braz. J. Microbiol. **34:**111–116.
9. **McCartney, M. R., U. Lins, M. Farina, P. R. Buseck, and R. B. Frankel.** 2001. Magnetic microstructure of bacterial magnetite by electron holography. Eur. J. Mineral. **13:**685–689.
10. **Spring, S., U. Lins, R. Amann, K.-H. Schleifer, L. C. S. Ferreira, D. M. S. Esquivel, and M. Farina.** 1998. Phylogenetic affiliation and ultrastructure of uncultured magnetic bacteria with unusually large magnetosomes. Arch. Microbiol. **169:**136–147.